Study of unsteady flow past a circular cylinder using a new computational approach at the outflow boundary

Syed Fahad Anwer, Nadeem Hasan, Sanjeev Sanghi*

Department of Applied Mechanics, Indian Institute of Technology, Delhi, New Delhi-110016, India

Abstract

This work presents a new procedure for extrapolating velocities at the outflow boundary from the interior in the computations of incompressible flows around rigid bodies. It has been demonstrated via numerical simulations of 2D, laminar, incompressible, viscous flow past a circular cylinder at Re = 100 and an impulsively started circular cylinder at Re = 550, that the usage of the proposed boundary condition allows one to limit the unbounded domain to a small size (6–8 times the characteristic size of the body) without any significant change in the flow characteristics like the lift coefficient (C_L) and the Strouhal number (St). Thus, the proposed boundary conditions can enhance the computational efficiency of this class of flows.

Keywords: Outflow boundary condition; CFD; SMAC; Cylinder; Uniform flow; Strouhal number; Convective boundary condition; Low Reynolds number; curvilinear coordinate system; Navier-Stokes equation

1. Introduction

In the CFD simulation of unsteady flow around a body in an open domain extending to infinity, the outflow conditions are often a source of problems. In steady flows, boundary conditions such as pressure being constant or a first derivative in the streamwise direction of any flow variable (pressure/velocity) is forced to zero. The computations involving NBC, however, require the placement of the outflow boundary at a large distance from the body in the downstream direction [1,2]. The outflow boundary in Okajima [1] and Stegall et al. [2] was placed at 125 and 100 times the characteristic size of the cylinder, respectively. Furthermore, it is known that for unsteady flows, such as the vortex shedding flow past bluff bodies, such conditions do not perform well and lead to distortion in the flow field near the outflow boundary.

The convective boundary condition (CBC) was proposed by Orlanski [3] for problems governed by a hyperbolic system of equations:

$$\frac{\partial \varphi}{\partial t} + \bar{u}\frac{\partial \varphi}{\partial n} = 0 \qquad (1)$$

where φ is any flow variable such as the velocity component and $\bar{u}$ is the convective velocity of flow structures, prescribed in a rather ad hoc way or by trial and error.

CBC has been used [4,5,6,7] in computing various flow configuration in two- and three-dimensional space. However, it is felt that CBC, besides lacking in a proper physical basis for elliptic and parabolic problems, is also somewhat awkward to implement. The quantity $\bar{u}$ is loosely defined in the literature as different authors have defined it in a different manner [4,5,6,7]. The value of $\bar{u}$, which yields minimum distortion in the vorticity structure at the exit, has to be determined by trial. A slightly different boundary condition has been used by Braza et al. [8]. The major drawback of this type of boundary condition is that a priori knowledge of the width of the wake on the outer boundary is needed for its application.

It is observed that the limitations of different types of boundary conditions employed by different workers are: (1) the numerical domain must extend a large distance downstream of the body, and (2) the application of the boundary condition involves guessing the value of some parameter (e.g. $\bar{u}$ in the CBC or width of the wake region [8]).

This work aims to circumvent these problems by providing an extrapolation procedure, which has a stronger physical basis and can be implemented in a

* Corresponding author. Tel.: +91 (11) 265 91 230; Fax: +91 (11) 265 81 119; E-mail: Sanghi@am.iitd.ernet.in

Computational Fluid and Solid Mechanics 2005
K.J. Bathe (Editor)

straightforward manner without any trial or guesswork. To demonstrate the validity of the procedure and to assess its performance, the problem of 2D, viscous, incompressible flow past a circular cylinder and impulsively started circular cylinder are considered. Numerical simulations have been carried out at Re = 100 and at Re = 550 for an impulsively started circular cylinder. This Re has been selected in order to demonstrate the performance of PBC in the unsteady, vortex shedding regime.

All numerical simulations have been carried out on a non-staggered, structured, curvilinear body fitted grid of O-type. The transformed Navier-Stokes equations have been discretized using the finite difference approach and a semi-explicit pressure correction algorithm is employed [9]. Numerical simulations for a circular cylinder have been carried out by placing the far field boundary at different distances from the body. A maximum distance of 20 and a minimum of 6 times the characteristic size of the body is employed for this purpose. This is done in order to know the extent to which the numerical domain can be limited in the usage of PBC and to quantitatively assess the effect of limiting the domain to progressively smaller dimensions. For different boundary placements, the Lift Coefficient (C_L), the Drag Coefficient (C_D), Strouhal number (St), vorticity and velocity fields near the exit and near the cylinder are compared.

2. Mathematical formulation

A procedure to exploit this radial behaviour in extrapolating the velocities from the interior to the outflow portion was developed by Karamchetti [10] and Hasan et al. [11]. Due to mass conservation, at infinitely large 'r', $(v_r - V_{r\infty})$ must behave at least as follows

$$(v_r - V_{r\infty}) \sim \frac{1}{r^2} \text{as } r \to \infty, \text{where } r = |\vec{r}| \tag{2}$$

and, due to negligible vorticity flux across the outermost layer of the computation, at infinitely large 'r', $(v_\theta - V_{\theta\infty})$ must behave as follows:

$$(v_\theta - V_{\theta\infty}) \sim \frac{1}{r^2} \quad \text{if } \Gamma = 0 \tag{3a}$$

$$(v_\theta - V_{\theta\infty}) \sim \frac{1}{r} \quad \text{if } \Gamma \neq 0 \tag{3b}$$

The working form of these equations are given as:

$$(v_r)_2 = \left\{\frac{r_1}{r_2}\right\}^2 (v_r)_1 + (V_{r\infty})_2 \left\{1 - \left(\frac{r_1}{r_2}\right)^2\right\} \tag{4}$$

Similarly,

$$\begin{aligned}(v_\theta)_2 &= \left\{\frac{r_1}{r_2}\right\}^2 (v_\theta)_1 + (V_{\theta\infty})_2 \left\{1 - \left(\frac{r_1}{r_2}\right)^2\right\} \text{ if } \Gamma_{r=r_1} = 0 \\ (v_\theta)_2 &= \left\{\frac{r_1}{r_2}\right\} (v_\theta)_1 + (V_{\theta\infty})_2 \left\{1 - \left(\frac{r_1}{r_2}\right)\right\} \text{ if } \Gamma_{r=r_1} \neq 0\end{aligned} \tag{5}$$

3. Governing equations and numerical scheme

An elliptic grid with an o-type of topology is generated around the body [12]. The simulations are carried out using a semi-explicit, pressure correction algorithm [9] similar to SMAC [13,14]. The solution for an impulsively started circular flow was obtained in an unconventional way. In the conventional way, the coordinate system is attached to the impulsively started cylinder and the transformed equation is then solved by any scheme. Here, the coordinate system was not attached to the moving cylinder and the flow was generated by moving the cylinder in a quiescent fluid. In this method, the grid has to be generated at every time step [12]. The equations are then transformed to a fixed computational plane and the time derivative is obtained in this plane. The movement of the physical plane is accounted for by the rate of change of x and y.

3.1. Boundary and initial conditions

On the outflow portion, the velocity is extrapolated from the interior using Eqs. (4) and (5) and pressure is obtained from Eq. (6) given by Gresho [15], where 'n' is the local normal direction at the boundary,

$$-P + 2\mu\left(\frac{\partial u_n}{\partial n}\right) = 0 \tag{6}$$

4. Results and discussion

A suitable outflow boundary condition for flows around immersed bodies should possess two important properties: (1) it should allow the flow to exit the domain with minimum distortion of the flow structure, and (2) it should permit the computations on a heavily truncated domain with negligible effect on the flow, as the artificial boundary is brought closer to the body. For problems involving an artificial boundary, introduced to truncate an otherwise infinite domain, it is of interest to examine the extent of truncation upto which a given outflow boundary condition retains these two properties. This has a direct bearing on the cost of computing such flows. In this section, the performance of PBC is examined in the context of the above mentioned criteria.

Table 1
The effect of far field boundary placement on Strouhal number and peak lift coefficient for uniform flow past circular cylinder at Re = 100

Far field boundary	Strouhal no. (St)	Peak lift coefficient (C_L)	Average drag coefficient ($\bar{C}_D$)
6D	0.1667	0.319	1.4239
8D	0.1667	0.307	1.3812
10D	0.1667	0.298	1.3581
12D	0.1667	0.305	1.3606
20D	0.1667	0.2958	1.3606
Numerical [8,13,17]	0.16	0.295	1.36
Experimental [16]	0.1667	–	–

4.1. Uniform flow past a circular cylinder (Re = 100)

To assess the performance of PBC, computations were carried out for uniform flow past a circular cylinder at Re = 100. The effect of shortening the outer boundary is studied by placing the outer boundary at distances of 6, 8, 10, 12 and 20D where 'D' is the characteristic size of the body. These grids have 121×124, 121×138, 121×148, 121×157 and 121×181 points respectively. A non-dimensional time step of 1×10^{-3} has been employed for all the cases. To ensure that the computations carried out for different levels of truncation of the flow domain reflect the effects of boundary placement only, the grid generated for the case of 20D is simply truncated and employed for the other cases. This ensures that the grid spacing remains the same for all the cases.

Table 1 shows the effect of placement of outflow boundary at 6D, 8D 10D, 12D and 20D for the case of circular cylinder at Re = 100. Here 'D' is the cylinder diameter. The parameters such as St and peak values of C_L are compared with the experimental and numerical values in [8] and [16]. It can be seen that as the outflow boundary is brought nearer to the cylinder from a distance of 20D to 6D, the deviations in the peak values of C_L from the value reported in [8] increase from 0.2% to 5%. However, there is no deviation in St and the values at different boundary placements match with those in [8] and [16]. The values of $\bar{C}_D$ match very well for the case of 20D with the data from [17]. The increase in $\bar{C}_D$ as the boundary is brought closer from a distance of 20D to 6D, over and above the value for 20D, is about 4.4%.

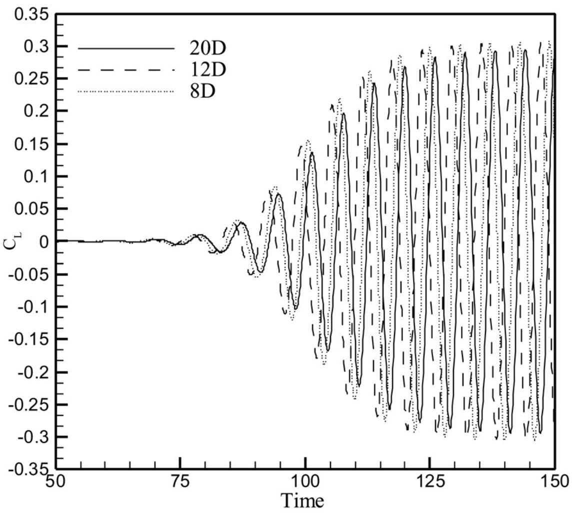

Fig. 1. Variation of coefficient of (C_L) at Re = 100 for different boundary placements for flow past a circular cylinder.

Figure 1 compares the time evolution of C_L for cases of 20D, 12D and 8D. It is interesting to observe that the growth rate and the frequency of the perturbations are not affected significantly. Only a phase shift is observed as the outer boundary is brought closer. This result is quite significant as it demonstrates that the usage of PBC on a heavily truncated domain does not significantly affect the amplitude growth rate and the oscillation frequency of the unstable mode or perturbation. The increase in the deviation observed in the peak values of C_L, as the outer boundary is brought closer to the body, is in any case inevitable as the outflow boundary conditions have been derived from the anticipated behaviour of the flow field at large distances.

Figures 2(a)–(d) show instantaneous vorticity and streamline contours in the wake region and near the exit for outer boundary placements at 6D, 8D, 12D and 20D at $\tau = 300$. It can be seen that there is no distortion of vortices near the exit as the outer boundary is brought closer from 20D to 6D. The phase shift mentioned earlier is clearly evident as the vortex is seen in different stages of the shedding cycle.

4.2. Impulsively started circular cylinder (Re = 550)

To test the performance of PBC on the flows which evolve due to the movement of the boundary, flow generated by an impulsively started circular cylinder at

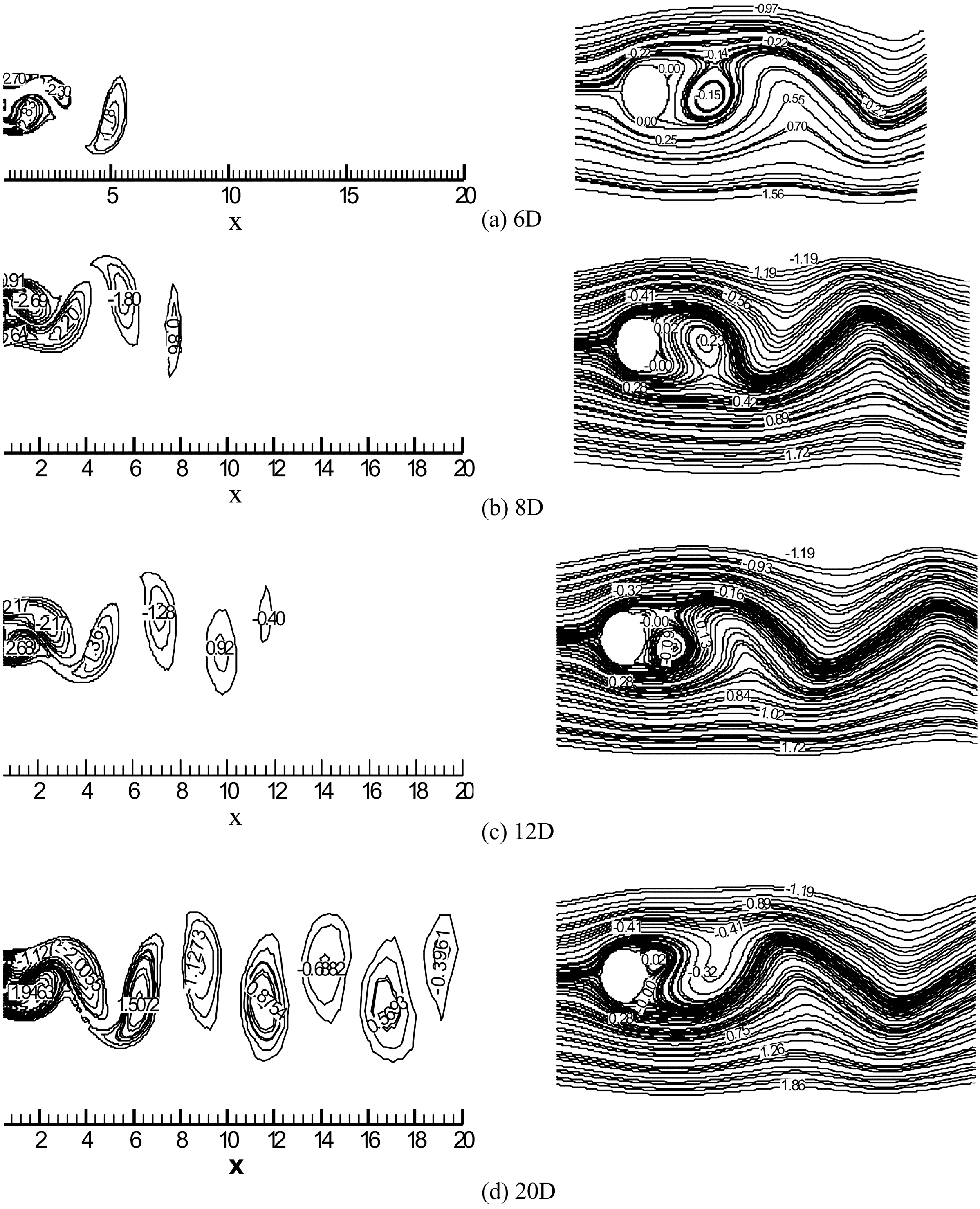

Fig. 2. Instantaneous vorticity and streamline contours for a circular cylinder in the wake for different boundary placements of (a) 6D (b) 8D (c) 12D (d) 20D at $\tau = 300$ for Re = 100.

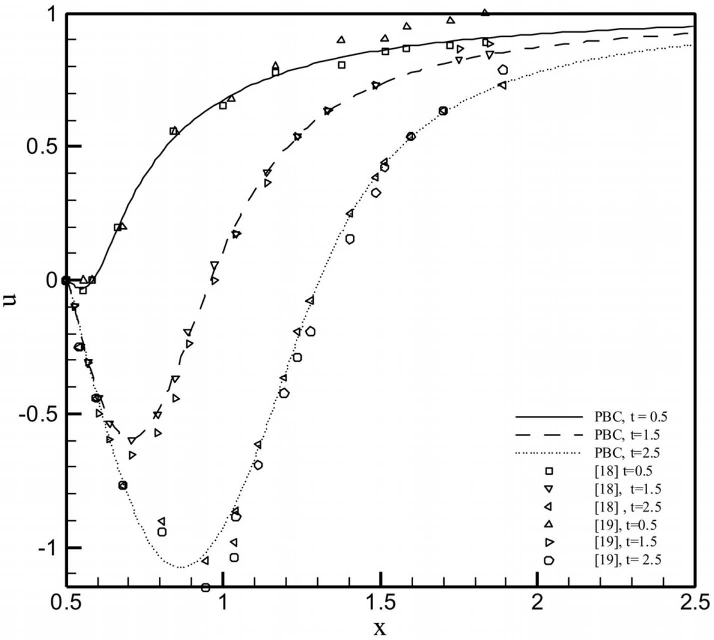

Fig. 3. Horizontal velocity at different locations along the x-axis in the wake at time instants of 0.5, 1.5 and 2.5 for an impulsively started circular cylinder at Re = 550.

Re = 550 is solved. The computations were done on grid with 161×181 points and with a time step of 1×10^{-4}. In Fig. 3, the results are compared with the numerical results of Wang [18], and experimental results generated by Boaurd et al. [19] are compared with the numerical results obtained by PBC. The agreement between computational results of PBC and Wang [18] is remarkably good but there is a deviation between experimental and numerical data due to the fact that the experiment is not strictly 2D.

5. Conclusions

In the present work, a new approach for handling outflow boundary condition based on the radial behavior of the velocity field at large distances from the body in external incompressible viscous flows has been presented. While the theoretical basis of this approach has been known for a long time [10], surprisingly it has not been used in numerical computations for such class of flows. It has been demonstrated that the numerical implementation of this methodology is quite straight forward. The validity and the performance of the method has been demonstrated through the classical problems of uniform flow past a circular and an impulsively started circular cylinder.

For this class of problems, it has been demonstrated that usage of PBC leads to accurate predictions even on a heavily truncated domain. Thus, the computational efficiency of such class of flows can be significantly enhanced by employing these boundary conditions.

References

[1] Okajima A. Strouhal numbers of rectangular cylinders. J Fluid Mech 1982;123:379–398.

[2] Stegell N, Rockliff N. Simulation of the effects of body shape on lock-in characteristics in pulsaring flow by the discrete vortex method. In: Proc of 3rd International Colloqium on Bluff body Aerodynamics and Applications, VA, 1996.

[3] Orlanski I. A simple boundary condition for unbounded hyperbolic flows. J Comput Phys 1976;21:251–269.

[4] Najjar FM, Vanka SP. Simulations of the unsteady separated flow past a normal plate. Int J Numer Methods Fluids 1995;21:525–547.

[5] Najjar FM, Balachandran S. Low frequency unsteadiness in the wake of a normal flat plate. J Fluid Mech 1998;370:101–147.

[6] Cheng L, Armfield S. A simplified marker and cell method for unsteady flows on non-staggered grids. Int J Numer Methods Fluids 1995;21:15–34.

[7] Pauley LL, Moin P, Reynolds WC. The structure of two-dimensional separation. J Fluid Mech 1990;220:307–441.

[8] Braza M, Chassing P, Minh HH. Numerical study and physical analysis of the pressure and velocity fields in the wake of a circular cylinder. J Fluid Mech 1986;165:79–130.

[9] Hirsch C. Numerical Computation of Internal and External Flows. Chichester: Wiley & Sons, 1990.

[10] Karamchetti K. Principles of Ideal Fluid Aerodynamics. New York: Wiley & Sons, 1966.

[11] Hasan N, Anwer SF, Sanghi S. On the outflow boundary condition for external incompressible flows: a new approach. In: Proc of 7th Annual CFD symposium, CFD Division of AeSI, 11–12 August, Bangalore, India, 2004.

[12] Shanks SP, Thompson JF. Numerical solution of the Navier Stokes equations for 2D hydrofoils in or below a free surface. Presented at the 2nd International Conference on Numerical Ship Hydrodynamics, Berkeley, CA, 1977.

[13] Rhie CM, Chow WL. Numerical study of the turbulent flow past an aerofoil with trailing edge separation. AIAA J 1983;21(7):1525–1532.

[14] Amsden AA, Harlow FH. The SMAC method: a numerical technique for calculating incompressible fluid flows. Los Alamos Scientific Report, LA 4370, 1970.

[15] Gresho PM. Incompressible fluid dynamics: some fundamental formulation issues. Ann Rev Fluid Mech 1991;23:413–454.

[16] Coutanceau M, Bouard R. Experimental determination of the main features of the viscous flow in the wake of a circular cylinder in uniform translation. Part 1. Steady flow. J Fluid Mech 1977;79:231–266.

[17] Barkley D, Henderson RD. Three dimensional floquet stability analysis of the wake of a circular cylinder. J Fluid Mech 1996;322:215–241.

[18] Wang J. Vortex generation and frequency selection in flapping flight. J Fluid Mech 2000;410:323–341.

[19] Board R, Coutanceau M. The early stage of development of the wake behind an impulsively started cylinder for $40 < Re < 10^4$. J Fluid Mech 2000;410:323–341.